

## RESEARCH ARTICLE

# The balancing act of *Nipponites mirabilis* (Nostoceratidae, Ammonoidea): Managing hydrostatics throughout a complex ontogeny

David J. Peterman<sup>1\*</sup>, Tomoyuki Mikami<sup>2</sup>, Shinya Inoue<sup>3</sup>

**1** Department of Geology and Geophysics, University of Utah, Salt Lake City, Utah, United States of America, **2** Department of Biological Sciences, University of Tokyo, Tokyo, Japan, **3** Hokkaido University, Shuma-nokai, Hokkaido, Japan

\* [sphenodiscus24@gmail.com](mailto:sphenodiscus24@gmail.com)



## Abstract

*Nipponites* is a heteromorph ammonoid with a complex and unique morphology that obscures its mode of life and ethology. The seemingly aberrant shell of this Late Cretaceous nostoceratid seems deleterious. However, hydrostatic simulations suggest that this morphology confers several advantages for exploiting a quasi-planktic mode of life. Virtual, 3D models of *Nipponites mirabilis* were used to compute various hydrostatic properties through 14 ontogenetic stages. At each stage, *Nipponites* had the capacity for neutral buoyancy and was not restricted to the seafloor. Throughout ontogeny, horizontally facing to upwardly facing soft body orientations were preferred at rest. These orientations were aided by the obliquity of the shell's ribs, which denote former positions of the aperture that were tilted from the growth direction of the shell. Static orientations were somewhat fixed, inferred by stability values that are slightly higher than extant *Nautilus*. The initial open-whorled, planispiral phase is well suited to horizontal backwards movement with little rocking. *Nipponites* then deviated from this bilaterally symmetric coiling pattern with a series of alternating U-shaped bends in the shell. This modification allows for proficient rotation about the vertical axis, while possibly maintaining the option for horizontal backwards movement by redirecting its hyponome. These particular hydrostatic properties likely result in a tradeoff between hydrodynamic streamlining, suggesting that *Nipponites* assumed a low energy lifestyle of slowly pirouetting in search for planktic prey. Each computed hydrostatic property influences the others in some way, suggesting that *Nipponites* maintained a delicate hydrostatic balancing act throughout its ontogeny in order to facilitate this mode of life.

## OPEN ACCESS

**Citation:** Peterman DJ, Mikami T, Inoue S (2020) The balancing act of *Nipponites mirabilis* (Nostoceratidae, Ammonoidea): Managing hydrostatics throughout a complex ontogeny. PLoS ONE 15(8): e0235180. <https://doi.org/10.1371/journal.pone.0235180>

**Editor:** Geerat J. Vermeij, University of California, UNITED STATES

**Received:** June 7, 2020

**Accepted:** July 22, 2020

**Published:** August 6, 2020

**Copyright:** © 2020 Peterman et al. This is an open access article distributed under the terms of the [Creative Commons Attribution License](https://creativecommons.org/licenses/by/4.0/), which permits unrestricted use, distribution, and reproduction in any medium, provided the original author and source are credited.

**Data Availability Statement:** Data are available from [https://www.morphosource.org/Detail/MediaDetail/Show/media\\_id/64314](https://www.morphosource.org/Detail/MediaDetail/Show/media_id/64314).

**Funding:** DP thanks the National Science Foundation (NSF-EAR-PF, #1952756) for some research materials and publication fees. SI and TM thank the Masason Foundation, the ANRI fellowship, and the JSPS (Japan Society for the Promotion of Science) KAKENHI (#18J21859) for funding a portion of this research. The funders had no role in study design, data collection and

## Introduction

Heteromorph ammonoids are ectocochleate cephalopods whose shells undergo changes in coiling throughout ontogeny. The seemingly aberrant shape of some heteromorph ammonoids piques curiosity about their enigmatic modes of life and life habit. Arguably, the most bizarre and conspicuous of all heteromorph genera is the Late Cretaceous (Turonian–Coniacian)

analysis, decision to publish, or preparation of the manuscript.

**Competing interests:** The authors have declared that no competing interests exist.

nostoceratid, *Nipponites* (Fig 1). Previous research has largely focused on the biostratigraphic usefulness of *Nipponites* [1–5] rather than its paleobiology [6, 7] and evolutionary significance [8]. The latter two areas are valuable because the morphology of this heteromorph appears deleterious to survival, seemingly defying the basic principles of natural selection [9–15]. It is more likely, however, that its functional morphology is obscured by a complex ontogenetic trajectory in shell growth. The shell of *Nipponites* is characterized by having several open planispiral (crioconic) whorls in early ontogeny, followed by a series of alternating U-bends around the earlier whorls (Fig 1); denoting some degree of regularity in coiling throughout a seemingly-aberrant ontogeny [1, 16, 17]. Okamoto [18–20] demonstrated that the coiling of

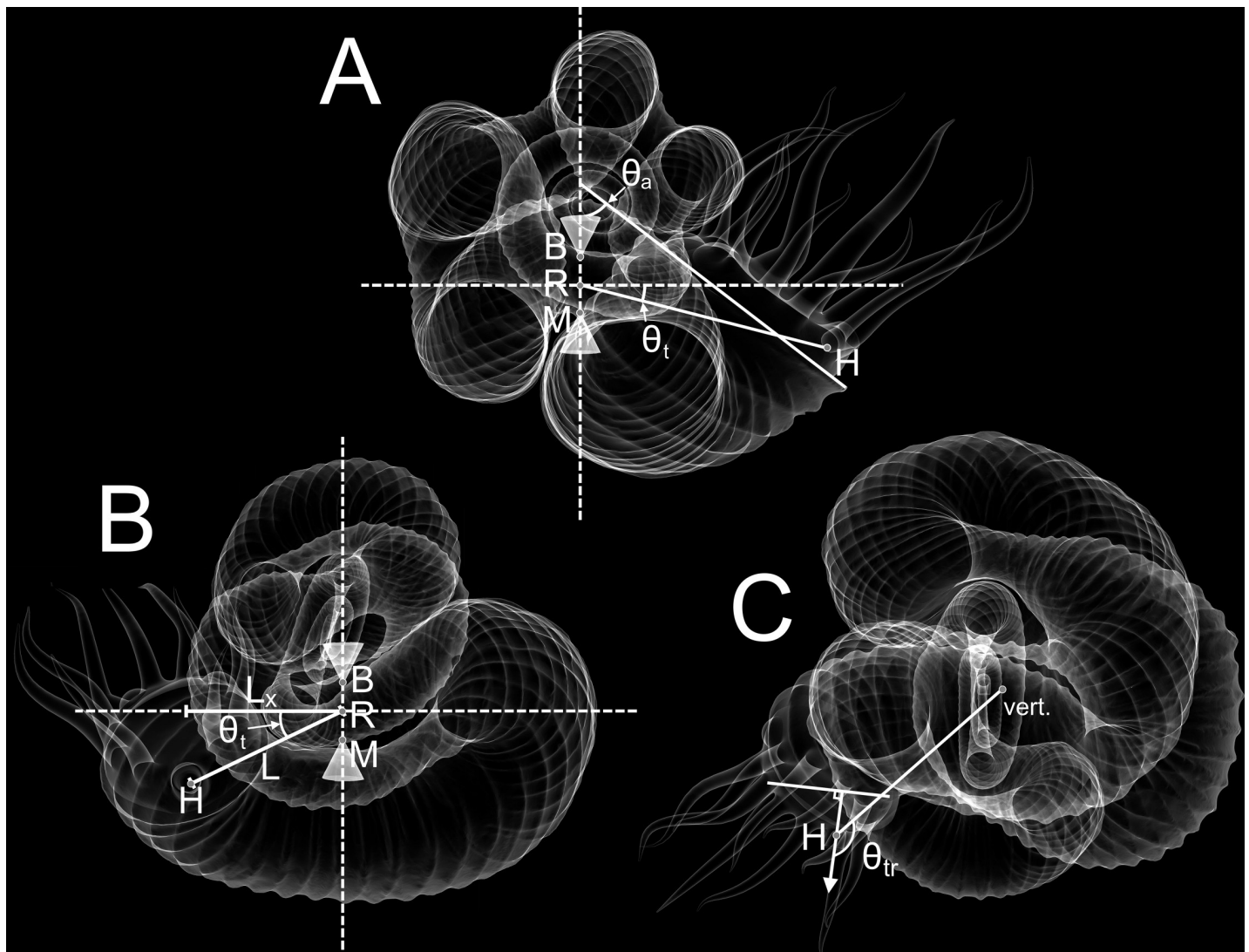


**Fig 1. Hydrostatic parameters of *Nipponites mirabilis*.** A, Side view of *Nipponites* in life position showing hypothetical centers of buoyancy (B), mass (M), and the horizontal axis of rotation (R). The angle of the aperture ( $\theta_a$ ) is measured as the inclination from the vertical plane. The thrust angle ( $\theta_t$ ) can be used to assess the directional efficiency of movement. This angle is measured between the horizontal plane, and a line passing through R and the location of the hyponome (source of thrust; H). B, Front view of *Nipponites* in life position facing the aperture. This view shows the total lever arm (L) and its x-component ( $L_x$ ) which is proportionate to the amount of rotational movement about the vertical axis produced during jet propulsion. C, Top view of *Nipponites* in life position showing the rotational thrust angle ( $\theta_{tr}$ ). This angle is measured between the vertical rotation axis (vert.), which passes through B and M, and the direction of the thrust vector (arrow emanating from H). Rotational thrust angles of  $90^\circ$  result in idealized transmission of thrust into pure rotation.

<https://doi.org/10.1371/journal.pone.0235180.g001>

*Nipponites mirabilis* is, in fact, well constrained and can be approximated by a few piecewise equations (alternations of sinistral and dextral helicoid phases surrounding the crioconic phase). Similarly, differential geometry has proven a useful tool in modeling these complex heteromorphs [21, 22]. The morphology of this genus varies from the more compact *N. mirabilis* to the less compact *N. occidentalis* and *N. bacchus* which both have more open whorls. The current study focuses on *N. mirabilis* unless otherwise stated. This iconic type species was chosen based on its regularity in coiling and the availability of data required to construct hydrostatic models.

The complex, meandering shell of *Nipponites* has invited several different interpretations regarding potential modes of life assumed by this heteromorph. The shell morphology of *Nipponites* has been compared to vermetid gastropods, and by analogy, this heteromorph has been suggested to assume a sessile and benthic mode of life [23–28]. Trueman [29] also considered *Nipponites* as benthic, but with some degree of mobility. Other nostoceratid genera have been interpreted as negatively buoyant, benthic organisms as well [28, 30, 31]. By similar analogy with other ‘irregularly-coiled’ mollusks, a symbiotic relationship with sponges or hydrozoans occupying the free space between the whorls of *Nipponites* has been speculated [32], although, no fossil evidence currently supports such a relationship. Contrasting benthic interpretations, Ward & Westermann [33] suggest that *Nipponites occidentalis* was capable of a planktic mode of life based on approximate calculations of organismal density. This mode of life is supported by Okamoto [19] for *Nipponites mirabilis* due to the oscillation of rib obliquity of the shell. Changes in rib obliquity suggests that some proper orientation of the soft body was preferred, which would not matter during a negatively buoyant condition. Favoring a planktic mode of life, Westermann [6] inferred that *Nipponites* was an occupant of the epipelagic, oceanic waters, perhaps as a vertical migrant or planktic drifter. Its morphology is certainly not streamlined, suggesting that it would have experienced considerably more hydrodynamic drag than its planispiral counterparts with similar whorl expansion and width. The unique shell of this genus raises questions regarding how its changes in coiling may reflect the modification of syn vivo hydrostatic properties. Such a tactic was suggested for other morphologies of heteromorph ammonoids [17, 19, 20, 34–39]. These physical properties are vital to understand if *Nipponites* was a benthic crawler, a planktic drifter, an active swimmer, or just an atypical genus with a morphology that was not detrimental for survival or reproduction. Ultimately, an investigation of this unique ammonoid can provide data to better understand heteromorph ammonoid modes of life, and perhaps, the selective pressures which may have acted on particular morphotypes.

## Hydrostatic properties of heteromorph ammonoids

The ability of ectocochleate cephalopods to attain neutral buoyancy is fundamental to reconstruct their modes of life. The variable interpretations for nostoceratid modes of life illustrate the importance of new techniques to determine the physical properties that would have acted on these living cephalopods. A neutrally buoyant condition is achieved when the total organismal mass is equal to the mass of the water displaced by the living animal. This depends upon the body chamber to phragmocone ratio. If the phragmocone (the chambered portion of the shell) is too small, the living cephalopod would not be able to compensate for its organismal weight and it would become negatively buoyant [34, 36, 40]. This condition also depends upon shell thickness and the densities assigned to each component of the living animal, which have been somewhat variable in previous research [39, 41].

Previous studies have demonstrated that heteromorph ammonoids may have been able to achieve much different life orientations than their planispiral counterparts, which are not

restricted to horizontal or diagonally-upwards soft body positions [20, 29, 34–39, 42–45]. These living cephalopods would have assumed some static orientation when their centers of buoyancy and mass were vertically aligned [41, 46, 47] (Fig 1). The difficulty to which these living cephalopods could deviate from their static orientation depends on hydrostatic stability, which is proportionate to the separation between the centers of buoyancy and mass [20]. High stability would have reduced the influence of external forms of energy on orientation, but would have simultaneously made it more difficult for the living cephalopod to self-modify its orientation [36].

The directional efficiency of movement (thrust angle) depends upon the relative position of the source of thrust (the hyponome) and the center of rotation (the midpoint between the centers of buoyancy and mass; Fig 1A and 1B). Thrust energy produced by jet propulsion is more efficiently transmitted into movement in the direction where the hyponome and center of rotation are aligned [20, 38, 39, 48, 49]. If these two points were horizontally aligned (thrust angle of zero), more energy would be transmitted to horizontal movement with minimal rocking. The rocking behavior of extant nautilids is related to their sub-horizontal thrust angles and the retraction of the soft body during emptying of the mantle cavity [50].

A rotational component of energy is increased by turning the direction of thrust out of alignment with the centers of buoyancy and mass (the axis where idealized rotation would occur; Fig 1B and 1C). An increased distance of the hyponome from these two centers would therefore produce a lever arm that would impart a torque to rotate the living cephalopod about its vertical axis. This type of movement is likely to have taken place for turrilitid heteromorphs [34], as well as other morphotypes with their apertures positioned in a similar relative manner [37]. Idealized rotation about the vertical axis would occur with a long, horizontally oriented lever arm and a thrust vector adjoining its distal end with a right angle.

Each of these physical properties would have significantly constrained the hydrostatic and hydrodynamic capabilities of living *Nipponites* throughout its ontogeny. Therefore, they provide fundamental information regarding the possible modes of life and life habit for this unique ammonoid, as well as possible adaptations for locomotion and feeding.

## Methods

Virtual models were constructed to determine the syn vivo hydrostatic properties of *Nipponites mirabilis*. Construction of the shell and other model components largely follow the methods of Peterman et al. [37–39], although a CT scanned specimen was used as the base model instead of using photogrammetry (similar to the methods of Morón-Alfonso [51]). This modification from the previous methods was preferred for this species due to the complex changes in shell ornamentation (rib obliquity). These ribs are parallel to the successive positions of the aperture throughout ontogeny, therefore retaining vital information about life orientation [20]. This method for virtual reconstruction is favorable for *Nipponites* because specimens of this genus are rarely found complete; discouraging destructive sampling techniques like serial grinding tomography [49, 56, 57]. Computed tomography (CT) scans of such specimens also lack contrasts of X-ray attenuation factors to distinguish the shell from its surrounding materials [52]. However, each of these tomographic techniques can provide very accurate measurements of hydrostatic properties and volumes when the specimens are adequate for imaging [52–59].

No permits were required for the described study, which complied with all relevant regulations.

## Virtual modeling of the shell

The shell of *Nipponites mirabilis* was constructed from an initial CT scan [60] of the specimen INM-4-346 (Museum Park Ibaraki Prefectural Museum of Nature; Ibaraki, Japan), which had



a remarkable degree of preservation. Most of the ontogeny is preserved in this specimen with minimal matrix on the inside (Fig 2A). However, two portions had to be virtually reconstructed; 1) the crushed ~5 cm section of the adoral-most part of the body chamber, and 2) the earliest crioconic whorls that are partially embedded in a remnant of the original concretion.

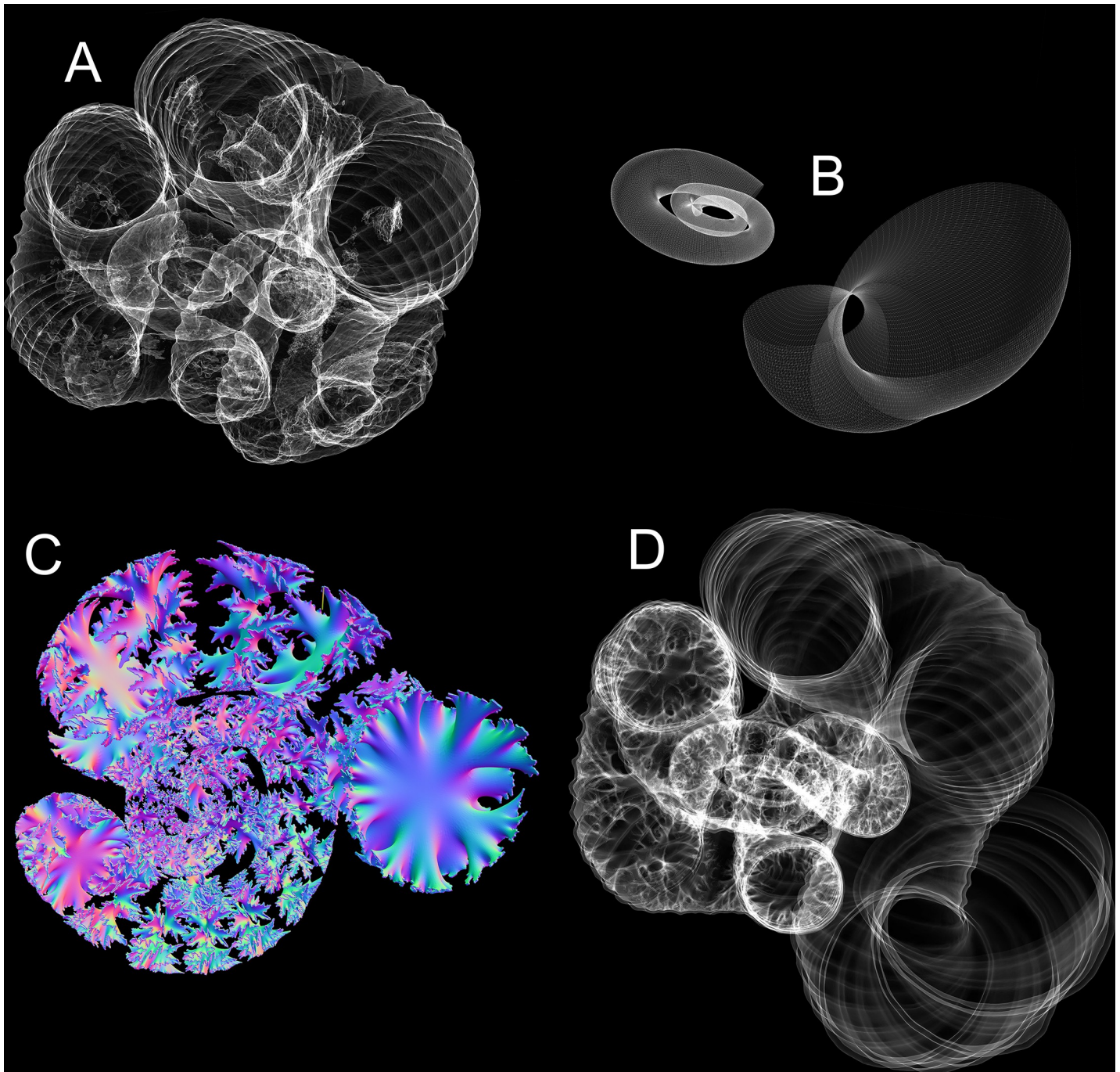


**Fig 2. Virtual reconstruction of the shell of *Nipponites mirabilis*.** A, Tessellated (.stl) 3D model generated from a CT-scan [60] of specimen INM-4-346. B, Reconstructed adoral portion of the body chamber and inner criocone phase with arrays algorithms (Table 1). C, Extruded septa generated from the suture pattern. D, Extruded shell and septa models unified together to produce a single, manifold 3D mesh of the entire shell.

<https://doi.org/10.1371/journal.pone.0235180.g002>

Table 1. Reconstruction of the shell.

Terminal Body Chamber		Translation (mm)			Rotation (degrees)			Scale		
Array #	# Replications	X	Y	Z	X	Y	Z	X	Y	Z
1*	67	-0.035	0.018	-0.265	-0.70	0.59	0.40	1.000	1.000	1.000
2*	29	-6.722	-6.548	-14.237	-0.70	1.00	-0.60	1.000	1.001	1.002
3*	40	-11.103	-12.910	-16.980	0.20	0.19	-1.70	1.002	0.999	1.001
Criocone Phase		Translation (mm)			Rotation (degrees)			Scale		
Array #	# Replications	X	Y	Z	X	Y	Z	X	Y	Z
1*	55	-30.050	-11.085	2.920	0.53	1.10	0.70	0.996	0.997	0.996
2	100	-30.057	-11.171	2.960	0.37	1.30	0.88	0.996	0.996	0.996
3*	122	-14.760	-14.063	5.757	0.39	0.88	0.69	0.998	0.998	0.998
4*	83	-25.009	-11.595	5.269	-0.15	1.80	0.70	0.997	0.997	0.997
5*	59	-20.306	-15.710	10.206	0.38	1.00	0.50	0.998	0.998	0.998
6	154	-20.286	-15.722	10.188	0.45	1.50	1.00	0.996	0.996	0.996

Array instructions used to reconstruct the juvenile criocone phase and the adoral portion of the terminal body chamber. These arrays were used in a piecewise manner to replicate the whorl section from the adoral direction to adapical direction by translation, rotation, and scaling in the x, y, and z directions. Asterisks denote arrays that had their origins reset to their current locations before replication. If origins were not reset, the origins of their previous arrays were used.

<https://doi.org/10.1371/journal.pone.0235180.t001>

These two portions of the shell were reconstructed (Fig 2B) with array algorithms [37–40], which replicate a whorl section and simultaneously translate, rotate, and scale it to build the shell from the adoral direction to adapical direction (Table 1). Such arrays are similar to the morphospace parameters of Raup [61]. The CT-scanned model [60] (which consists of a stack of.tiff images) was converted to the tessellated.stl format required for model reconstruction and volumetry using the program Molcer 1.51 [62]. The external mesh of the tessellated file was isolated in order to get rid of internal features like fissures and X-ray attenuation artifacts. External defects were smoothed in Meshmixer 3.3 [63] while maintaining the curvature of neighboring, complete features. This external 3D-mesh served as a stencil for the reconstruction of the missing and damaged portions of the shell. After the missing portions of the shell were combined to the model derived from the CT-scan, the ornamentation was reconstructed by matching the width and amplitude of ribs with a torus shape in Blender [64], then properly oriented using the ribs present on the inner whorls. The ornamentation, reconstructed portions of the shell (Fig 2B), and the total external mesh were repaired and unified in Netfabb [65] to produce a single manifold mesh of the exterior shell. The program Blender was used to assign shell thickness to the external shell model based on measurements from specimen NMNS (National Museum of Nature and Science; Tokyo, Japan) PM35490 (Fig 3), producing a mesh denoting the entire shell without septa.

Septa were constructed by recording a suture pattern from specimen NMNS PM35490 (Fig 4). The external shell of this specimen (Fig 4B and 4C) was removed with air abrasives and pneumatic tools under a stereoscopic microscope and the suture (Fig 4D) was recorded with a digital camera lucida. This suture was imported in the Blender workspace and the curve modifier was used to wrap it around the whorl section of the shell. This suture was then replicated and placed along the majority of the phragmocone so that adjacent lobules and folioles were almost tangential. Ontogenetic changes in the suture pattern were not considered because they probably represent only small differences in mass and its distribution. That is, each suture had the same degree of complexity and its expanded portion was placed adjacent to the venter throughout ontogeny. The crioconic, bilaterally symmetric juvenile phase was reconstructed with array algorithms, which allowed septa to be duplicated with the same equations. The

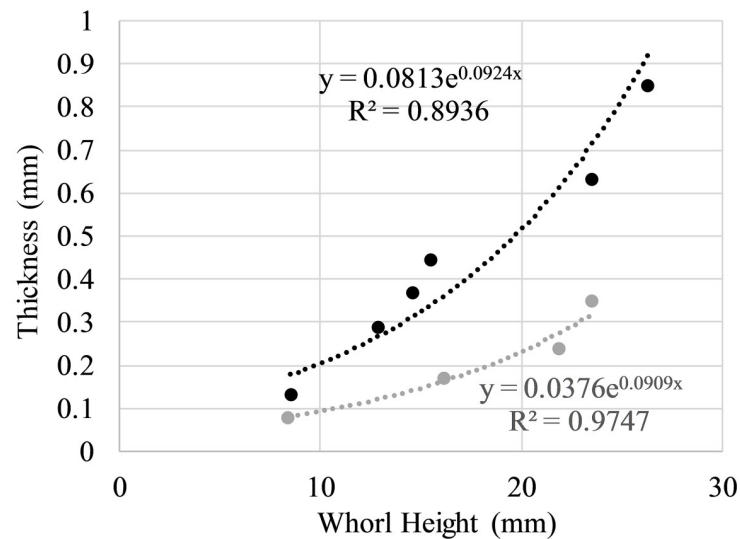


**Fig 3. Thickness measurements used for virtual model extrusion.** Thicknesses of the shell (black) and septa (grey) as a function of whorl height. Measurements were recorded from specimen NMNS PM35490 and used to define thickness in the virtual model.

<https://doi.org/10.1371/journal.pone.0235180.g003>

septa within the majority of the phragmocone were constructed by extruding the suture patterns inwards to a single point, then refining and smoothing the interior in order to approximate minimum curvature surfaces. A body chamber ratio of approximately 42% the total curvilinear length was measured from a remarkably complete specimen of *Nipponites mirabilis* from a private collection. This specimen was 3D scanned with an Artec Space Spider (to allow comparisons with the CT scanned specimen) and is housed in the morphosource database [66]. A nearly complete specimen of *Nipponites mirabilis* (MCM-A0435; Mikasa City Museum, Mikasa, Japan; Fig 4E) was also compared in this manner and stored in the database [66], which yielded an approximate body chamber ratio of 36%. This ratio would be slightly higher if the aperture was not partially crushed. The proper number of septa to maintain the body chamber ratio of around 42% were placed in the phragmocone and extruded based on measured thicknesses from specimen NMNS PM35490 (Fig 3). These final septa (Fig 2C) were merged with the extruded, external shell to produce a single, manifold 3D mesh of the entire, septate shell (Fig 2D).

### Virtual modeling of the soft body and camerae

The shell constrains the size and shape of other model components that influence hydrostatics. A model of the soft body was constructed by isolating the interface between the shell and the body chamber, and similarly, the camerae were isolated from the phragmocone of the shell. The faces of the isolated body chamber and camerae meshes were inverted so that the normals (vectors denoting the outside) were pointed outwards. The ammonoid soft body is largely unknown; however, due to phylogenetic bracketing [67], the presence of ten arms can be inferred [68–70] with a possibly reduced (compact) soft body. A soft body resembling the consensus of Klug & Lehmann [70] and Landman et al. [71] was constructed for *Nipponites* and unified to the repaired, isolated internal body chamber mesh. The camerae were later partitioned into fractions of cameral liquid and cameral gas for hydrostatic calculations. For the sake of model simplicity, both cameral liquid and cameral gas were assumed be evenly



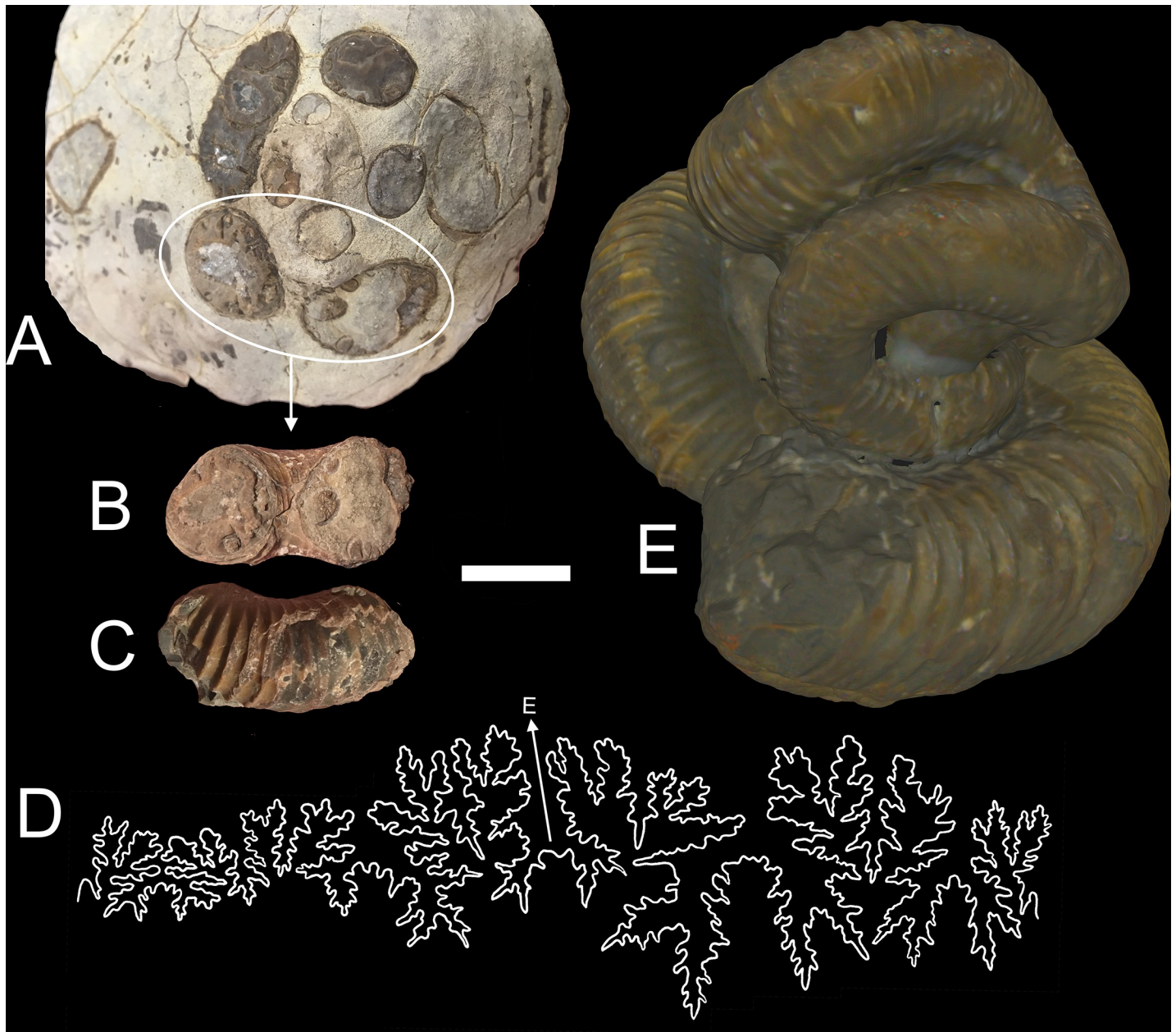


**Fig 4. Specimens used for shell reconstruction.** A, Original concretion containing NMNS PM35490. Umbilical view (B) and ventral view (C) of the shell section used to record the suture pattern (D). E, 3D scan of the Mikasa City Museum Specimen (MCM-A0435) used to approximate the body chamber ratio. Scale bar = 2 cm.

<https://doi.org/10.1371/journal.pone.0235180.g004>

distributed in the phragmocone. This assumption may be reasonable based on the retention of cameral liquid via the pellicle and surface tension along septal margins [72]. However, the distribution of cameral liquid likely changed throughout ontogeny, having been located behind the soft body as new septa formed. The hydrostatic influence of this assumption is small as long as the percentage of cameral liquid in the phragmocone is low. This process yielded mass distributions of the fractions of cameral liquid and cameral gas that have the same centers as the center of volume for all camerae.



## Modeling changes in shell morphology throughout ontogeny

The final hydrostatic model of the adult *Nipponites mirabilis* was used to derive a total of 14 models representing different ontogenetic stages. This was accomplished by deleting the septa in the phragmocone and deleting the adoral portion of the body chamber so that the proper body chamber ratio was maintained throughout ontogeny. The apertures of these stages were chosen to terminate near the apices and inflection points between the U bends of the shell in order to sample a variety of former aperture positions. The total curvilinear distance along the venter from the apex to the aperture was normalized by this same distance for the terminal stage, yielding a proxy for the age of each model. This distance was measured virtually in Blender, by isolating a curved line along the venter in 3D space and measuring the sum of the tens of thousands of straight line segments that closely approximate this curve. Such a metric for age is only an estimate because both absolute and relative time cannot be quantified. Therefore, the normalized value reported is relative, and represents the percentage of the way through an individual's lifespan if the shell's linear growth rate is held constant. It is unknown how this growth rate changes throughout ontogeny, but it likely would have changed in some way. It is also possible that the body chamber ratio of *Nipponites* subtly changed throughout ontogeny, which has been reported for other ammonoids [73].

## Hydrostatic calculations

Neutral buoyancy occurs when the sum of organismal mass is equal to the mass of water displaced. The proportion of camerae to be emptied of cameral liquid relative to the total available cameral volume ( $\Phi$ ) that satisfies a neutrally buoyant condition was computed with the following equation (after Peterman et al., 2019a):

$$\Phi = \frac{\left( \frac{V_{wd}\rho_{wd} - V_{sb}\rho_{sb} - V_{sh}\rho_{sh}}{V_{ct}} \right) - (\rho_{cl})}{(\rho_{cg} - \rho_{cl})} \quad (1)$$

Where  $V_{wd}$  and  $\rho_{wd}$  are the volume and density of the water displaced,  $V_{sb}$  and  $\rho_{sb}$  are the volume and density of the soft body,  $V_{sh}$  and  $\rho_{sh}$  are the volume and density of the shell,  $\rho_{cl}$  is the density of cameral liquid,  $\rho_{cg}$  is the density of cameral gas, and  $V_{ct}$  is the total cameral volume of the phragmocone. A soft body density of 1.049 g/cm<sup>3</sup> is preferred based on the measurement of *Nautilus* soft body by Hoffmann & Zachow [74] that was later averaged by a seawater-filled mantle cavity and thin mouthparts by Peterman et al. [38]. A shell density of 2.54 g/cm<sup>3</sup> was adopted from Hoffman & Zachow [74]. The cameral liquid density of 1.025 g/cm<sup>3</sup> [75] and cameral gas density of 0.001 g/cm<sup>3</sup> are used in the current study.

The total center of mass is weighted according to each material of unique density (i.e., the soft body, shell, cameral liquid, and cameral gas in the current study). Each individual center of mass for the soft body, shell, cameral liquid, and cameral gas were computed in MeshLab [76] and the total center of mass was computed with the equation:

$$M = \frac{\sum(L * m_o)}{\sum m_o} \quad (2)$$

Where  $M$  is the total center of mass in a principal direction,  $L$  is the center of mass of a single object measured with respect to an arbitrary datum in each principal direction, and  $m_o$  is the mass of any particular object that has a unique density. Eq 2 was used in the x, y, and z directions to compute the coordinate position of the center of mass.

The center of buoyancy ( $B$ ) is equal to the center of volume of the medium displaced by the external model. A model denoting the exterior interface of *Nipponites* was constructed from

the external shell and soft body protruding from the aperture and its center was computed in MeshLab.

The static orientation of the total model occurs when B and M are vertically aligned. The hydrostatic stability index is computed from these centers.

$$S_t = \frac{|B - M|}{\sqrt[3]{V}} \quad (3)$$

The separation between the centers of buoyancy (B) and mass (M) is normalized by the cube root of the organismal volume (V; equal to the volume of seawater displaced) in order to be applied to ectocochleates with irregular coiling [20].

Apertural angles ( $\theta_a$ ) were measured with respect to the vertical (Fig 1A). That is, angles of zero correspond to a horizontally facing soft body, angles of +90° correspond to an upward facing soft body, and angles of -90° correspond to a downward facing soft body.

Thrust angles ( $\theta_t$ ) were measured with respect to the horizontal (Fig 1B) between the point source of thrust and the rotational axis. Therefore, as the thrust angle approaches zero, more energy is transmitted into horizontal movement with a lower rotational component.

Rotational thrust angles ( $\theta_{tr}$ ) were measured between the thrust vector (perpendicular to the aperture) and the rotational axis (Fig 1C). A rotational thrust angle of 90° would allow pure rotation to take place, while angles of 0° and 180° would result in translational movement.

## Results

The unknown soft body can produce errors in buoyancy calculations depending upon its total volume. By comparing the soft body used herein with a soft body that terminates at the aperture, there is only a 0.5% difference in the proportion of the phragmocone to be emptied for neutral buoyancy ( $\Phi$ ). Similarly, the mass distribution is not significantly different between either model (a 0.7% difference in hydrostatic stability), partially because the soft body density is similar to that of seawater.

Because the body chamber ratio was somewhat variable (~6% different) on measured specimens, this ratio was manipulated by removing one septum and adding one septum to the terminal stage model with a body chamber ratio of 42%. Removing one septum increases the total body chamber ratio to 46%. This change yields a 16% increase in  $\Phi$  (to 84.6%) and a 7% increase in  $S_t$  (to 0.0786). Adding one septum decreases the body chamber ratio to 37%, yielding a 10% decrease in  $\Phi$  (to 65.7%) and an 8% decrease in  $S_t$  (to 0.0676). These changes suggest that a small error (~10%) in body chamber ratio would not significantly alter calculations of buoyancy or the characteristics of the mass distribution. Small deviations from the ideal body chamber ratio took place (Table 2) during model construction. However, the body chamber ratio test suggests that their hydrostatic influences are minimal. Similarly, changes in the true body chamber ratio throughout ontogeny would result in minimal error if such differences were sufficiently low (approximately less than 10%).

The densities assumed in the hydrostatic calculations could potentially adjust the total mass and its distribution, therefore, directly influence the conditions for neutral buoyancy ( $\Phi$ ) and hydrostatic stability ( $S_t$ ). Using historically higher density values for the soft body with an estimate of aptychi (1.068 g/cm<sup>3</sup> [38]) and the shell (2.62 g/cm<sup>3</sup> [36]),  $\Phi$  is increased by 9.9% and  $S_t$  is increased by 11.9%. While values of 1.049 g/cm<sup>3</sup> and 2.54 g/cm<sup>3</sup> are preferred for the soft body and shell, respectively [38], this test demonstrates that hydrostatic calculations are sensitive to density values, which have varied historically [41].

Table 2. Hydrostatic properties of *Nipponites mirabilis*.

Stage	Age (%)	BC Ratio	$\Phi$	$S_t$	$\theta_a$	$\theta_{ao}$	L (mm)	$L_x$ (mm)	L norm	$L_x$ norm	$\theta_t$	$\theta_{tr}$
(Crio) 1	0.18	42.7	97.3	0.099	69.5	69.0	11.65	11.43	1.236	1.212	11.1	7.7
2	0.23	38.6	82.6	0.101	74.3	49.5	10.59	10.59	0.902	0.902	1.0	117.8
3	0.29	40.1	83.5	0.094	13.8	14.5	10.04	9.43	0.726	0.682	-20.1	117.1
4	0.33	39.7	76.4	0.093	99.5	99.5	9.58	8.61	0.616	0.554	26.0	98.2
5	0.38	42.8	77.4	0.069	2.0	-30.3	13.28	11.19	0.773	0.651	-32.6	135.5
6	0.41	42.7	75.5	0.082	22.9	24.1	14.61	12.23	0.787	0.659	-33.1	139.1
7	0.49	42.6	81.7	0.070	24.1	5.0	16.64	14.32	0.765	0.658	-30.6	124.5
8	0.55	41.6	79.8	0.083	31.5	22.4	19.51	16.20	0.821	0.682	-33.9	143.0
9	0.60	42.2	79.8	0.083	31.6	18.8	18.88	16.49	0.753	0.658	-29.1	113.4
10	0.71	41.8	81.3	0.079	34.5	15.1	21.92	21.72	0.758	0.752	-7.6	123.2
11	0.77	41.2	76.3	0.075	17.3	-12.7	22.18	17.38	0.720	0.564	-38.4	122.0
12	0.83	43.5	75.4	0.076	50.1	39.8	27.54	27.38	0.835	0.830	-6.2	154.2
13	0.88	39.1	72.2	0.072	-8.2	-11.1	27.66	24.86	0.807	0.726	-26.0	105.9
(Term) 14	1.00	42.1	73.1	0.073	19.9	30.0	28.10	23.44	0.781	0.651	-33.5	131.1

Hydrostatic properties computed for the 14 ontogenetic stages examined. Crio = criocone phase; Term = terminal phase; Age% = curvilinear length for that stage normalized by the curvilinear length of the terminal specimen; BC Ratio = curvilinear length of body chamber normalized by the total curvilinear length at a particular stage;  $\Phi$  = the proportion of the phragmocone to be emptied of liquid for a neutrally buoyant condition;  $S_t$  = hydrostatic stability index;  $\theta_a$  = apertural angle;  $\theta_{ao}$  = apertural orientation if rib obliquity was ignored (normal to shell growth direction); L = total lever arm;  $L_x$  = x-component of the lever arm, norm = normalized by the cube root of water displaced for each particular stage;  $\theta_t$  = thrust angle;  $\theta_{tr}$  = rotational thrust angle.

<https://doi.org/10.1371/journal.pone.0235180.t002>

The number of septa in the phragmocone and their positions were based on a single septum constructed from a suture pattern in the adapertural region of the adult phragmocone. Variability in septal morphology throughout ontogeny could have resulted in an inappropriate number of septa, which would have altered shell mass. To better understand the influence of this assumption, five septa from the middle of the phragmocone (whorl height of ~1 cm) were added and subtracted from the final adult model. This modification resulted in minor differences of about  $\pm 1.7\%$  in  $\Phi$  and  $\pm 1.5\%$  in  $S_t$  (similar to the experiment of Hoffmann et al. [53])

## Ontogenetic changes in hydrostatics

Hydrostatic properties were computed for 14 life stages (Figs 5 and 6; Table 2) in order to assess changes throughout the ontogeny of *Nipponites mirabilis* and other species sharing similar morphologies. *Nipponites mirabilis* has the capacity for neutral buoyancy at all life stages, retaining liquid between approximately 3% and 28% of the total cameral volumes. After the juvenile criocone phase,  $\Phi$  decreases and stabilizes at its lower values (Fig 7). Hydrostatic stability ( $S_t$ ) follows a similar decreasing trend and does not significantly oscillate (Fig 7). These hydrostatic stability index values ranging between approximately 0.10 and 0.07 are sufficiently large enough to orient the living cephalopod to maintain some static orientation during all of the examined ontogenetic stages. As already suggested by Okamoto [20, 21], the orientation of the aperture ( $\theta_a$ ) oscillates in a complicated fashion throughout ontogeny, ranging between approximately -11 and 99 degrees in the current study (Fig 7). Apertural orientations significantly turned downwards are not observed. The juvenile criocone phase has apertural angles of about 70°, followed by complex oscillations as the alternating U-shaped bends develop. Afterwards, there is some degree of regularity in orientation, mostly exhibiting horizontal and

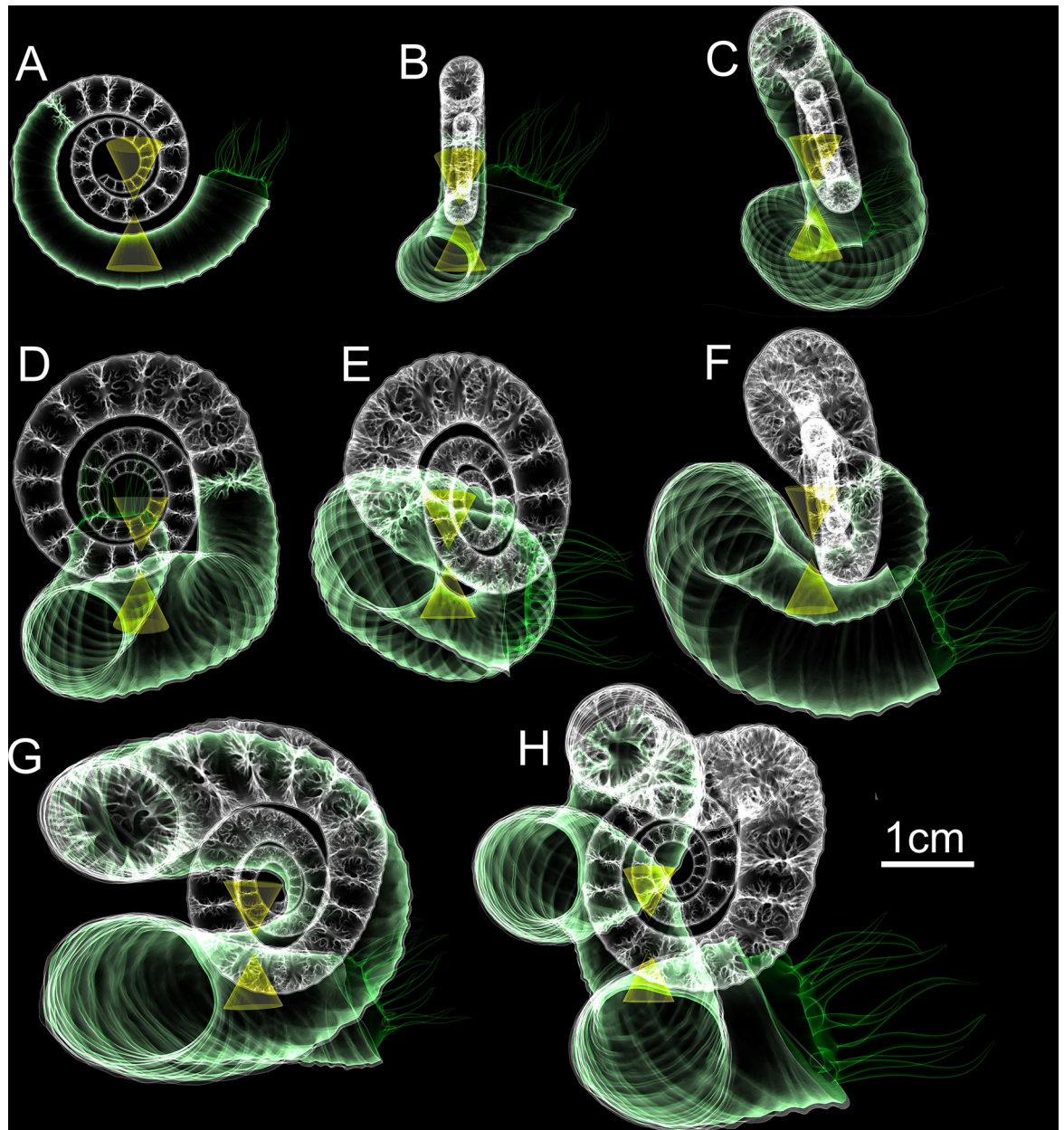


**Fig 5.** Final hydrostatic models of the first eight ontogenetic stages (A-H) of *Nipponites mirabilis*. All models are oriented so that the ventral margin of the aperture faces towards the right. The tip of the upper cone corresponds to the center of buoyancy while the tip of the lower cone is the center of mass. At rest, these two centers are vertically aligned, denoting the proper static orientation assumed by living *Nipponites mirabilis*.

<https://doi.org/10.1371/journal.pone.0235180.g005>

diagonally upwards directions (Fig 7). These properties likely vary, based on the possibility of a slightly changing body chamber ratio throughout ontogeny.

### Rib obliquity and static orientation

While apertural orientations during the ontogeny of *Nipponites mirabilis* vary, horizontal to upward orientations are preferred. This is further supported by comparing the apertural angles (as denoted by the orientation of the ribs on the shell) with the same angle if ribs were not



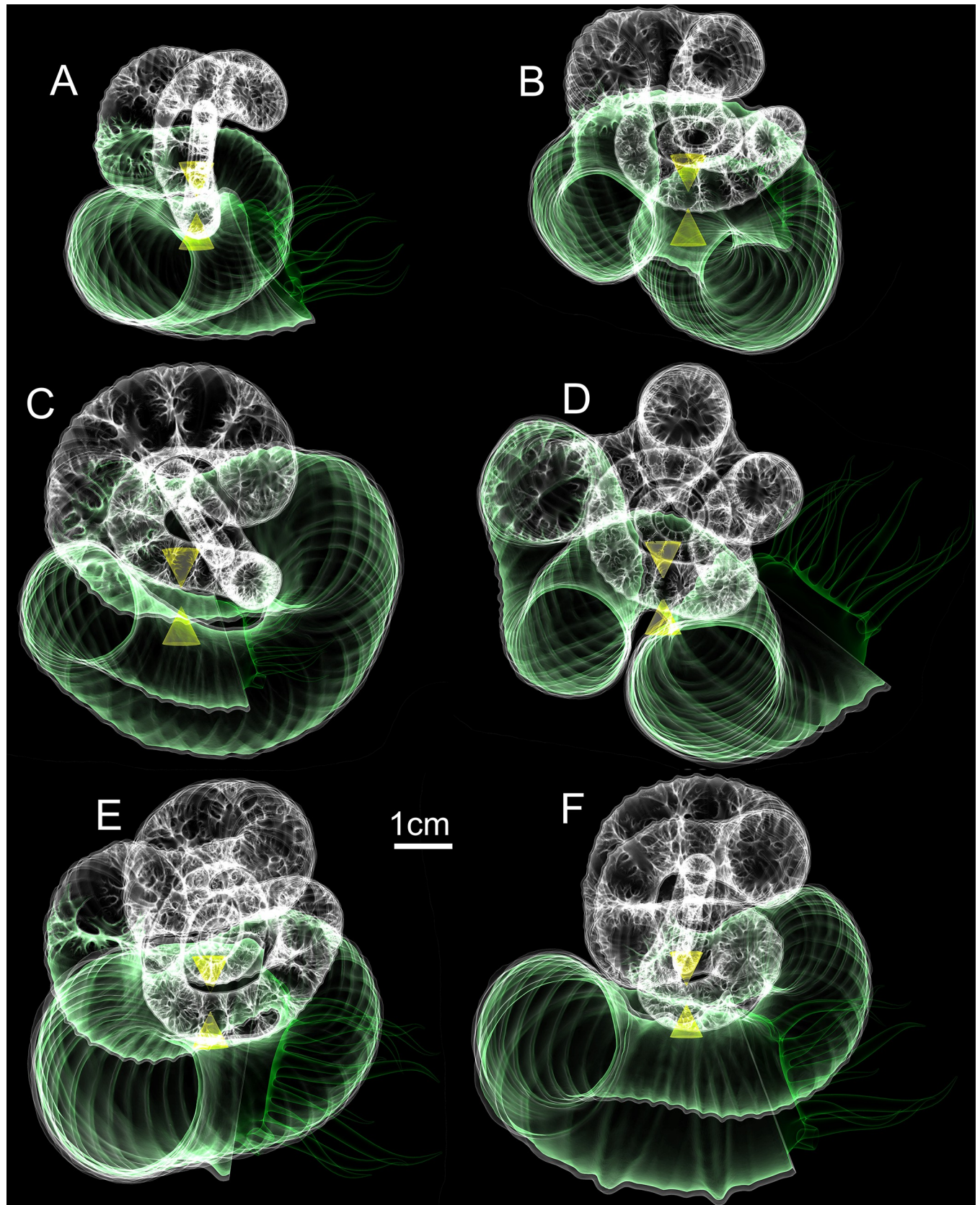


**Fig 6.** Final hydrostatic models of the last six ontogenetic stages (A-F) of *Nipponites mirabilis*. All models are oriented so that the ventral margin of the aperture faces towards the right. The tip of the upper cone corresponds to the center of buoyancy while the tip of the lower cone is the center of mass. At rest, these two centers are vertically aligned, denoting the proper static orientation assumed by living *Nipponites mirabilis*.

<https://doi.org/10.1371/journal.pone.0235180.g006>

oblique (i.e., if the aperture was perfectly perpendicular to the direction of shell growth). The obliquity of the ribs generally enhances the apertural orientation by about  $10^\circ$  in the upwards direction (Fig 8). Unless otherwise stated, the apertural angles reported herein are measured parallel to the ribs and represent the aperture positions that would have occurred during life at each ontogenetic stage.

### Directional efficiency of movement

During its juvenile crioconic phase, *Nipponites mirabilis* was well suited for horizontal backwards movement (denoted by the near zero thrust angles;  $\theta_v$ ). This trend somewhat persists into later ontogenetic stages, while slightly decreasing and remaining above  $-40^\circ$ . However, after the crioconic phase, the rotational thrust angle ( $\theta_{tr}$ ) dramatically increases as the U-shaped bends in the shell develop, suggesting that there is a strong rotational component of movement when thrust is produced normal to the aperture (Fig 9). While the normalized lever arm lengths seem to decrease during ontogeny, sufficient torques for rotation can only be produced when the rotational thrust angle is high. Furthermore, the x-component of the normalized lever arm is not significantly lower than the total normalized lever arm during ontogeny, suggesting that the subhorizontal declination of the total lever arms would still provide significant rotational movement in ontogenetic stages after the crioconic phase (Fig 9).

## Discussion

### The mode of life of *Nipponites*

Hydrostatic simulations reveal that *Nipponites mirabilis* had the capacity for neutral buoyancy throughout its ontogeny ( $\Phi$  values  $< 100\%$ ), retaining some amount of cameral liquid in the

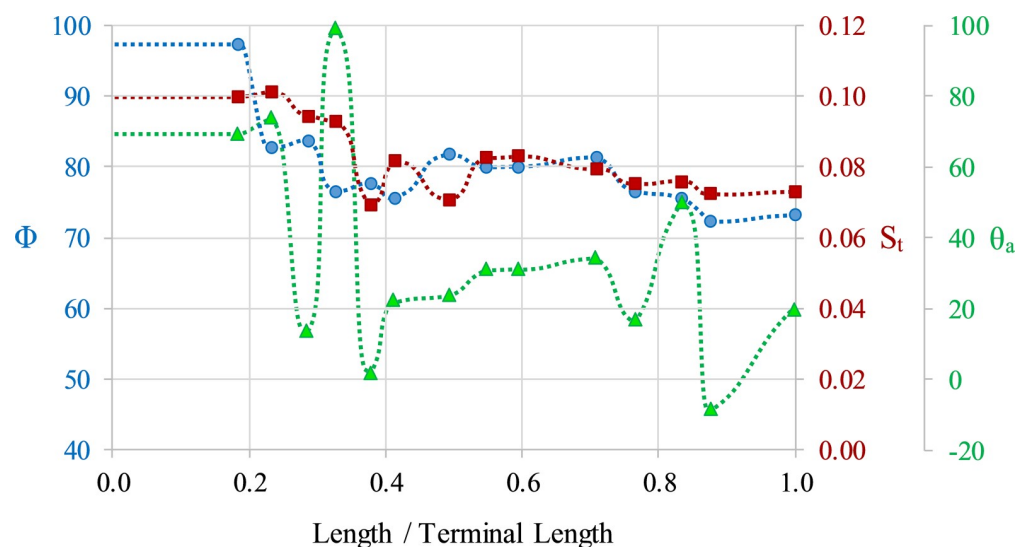


**Fig 7. Hydrostatic properties computed throughout ontogeny.** The proportion of the phragmocone to be emptied of cameral liquid for neutral buoyancy ( $\Phi$ ; circles), hydrostatic stability index ( $S_t$ ; squares), and apertural angles ( $\theta_a$ ; triangles) as a function of age (proxied by the curvilinear length for that stage normalized by the curvilinear length of the terminal specimen). Dashed lines denote interpolations between the 14 measured stages.

<https://doi.org/10.1371/journal.pone.0235180.g007>

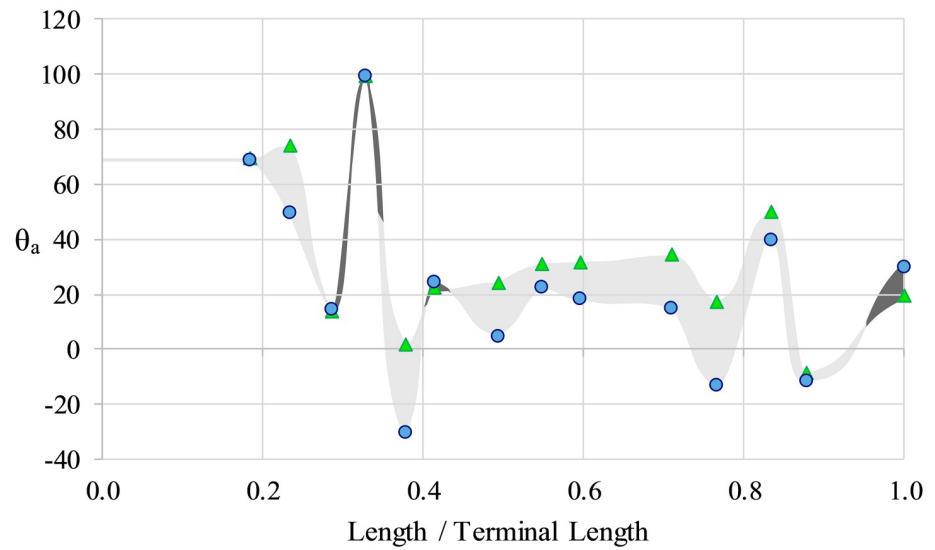


**Fig 8. The influence of rib obliquity on orientation.** Apertural angles with observed rib obliquity ( $\theta_a$ ; triangles) and the angles normal to the direction of shell growth (zero obliquity; circles) as a function of age (proxied by the curvilinear length for that stage normalized by the curvilinear length of the terminal specimen). Light grey shading and dark grey shading denote rib obliquity that boosts  $\theta_a$  in the upwards direction and downward directions, respectively.

<https://doi.org/10.1371/journal.pone.0235180.g008>

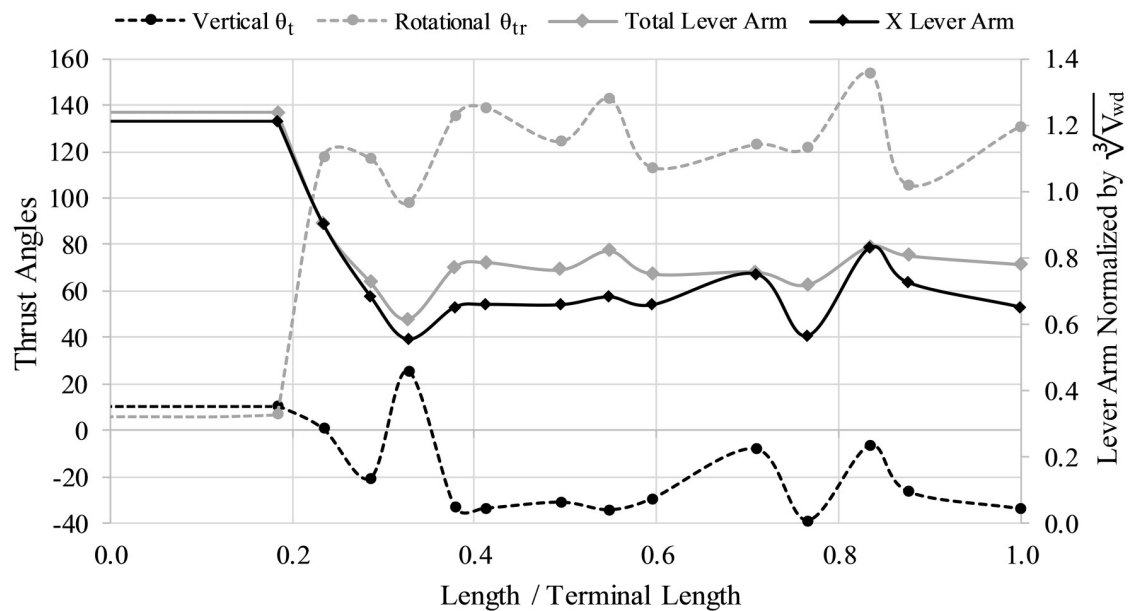


**Fig 9. The directional efficiency of movement.** Thrust angles in the vertical direction ( $\theta_t$ ; black dashed line), rotational thrust angles ( $\theta_{tr}$ ; grey dashed line), and lever arms as a function of age (proxied by the curvilinear length for that stage normalized by the curvilinear length of the terminal specimen). The total lever arm (grey solid line) and x-component of that lever arm (X Lever Arm; solid black line) are both normalized by the cube root of the volume of water displaced ( $V_{wd}$ ) for each stage. Idealized rotation would take place with high, relative x-components of the lever arm and  $\theta_{tr}$  of  $90^\circ$ . Idealized horizontal movement would occur with  $\theta_t$  of  $0^\circ$  and  $\theta_{tr}$  of  $0^\circ$  or  $180^\circ$ .

<https://doi.org/10.1371/journal.pone.0235180.g009>



shell to compensate for residual buoyancy (Fig 7). These results support the buoyancy calculations of Ward and Westermann [33], who report a similar scenario for *N. occidentalis*. The inferences drawn from rib obliquity most likely functioning in a neutrally buoyant setting [19] are also supported by the hydrostatic results. While the coiling of *Nipponites* is complex and somewhat resembles gastropods such as vermetids and *Opisthostoma* [23–27], considerable negative buoyancy and resultant benthic modes of life are unlikely.

Hydrostatic stability is large enough for living *Nipponites* to assume static, syn vivo orientations throughout its entire ontogeny (excluding some short time after hatching when the relative effects of viscous forces are higher). While the hydrostatic stability index slightly decreases throughout ontogeny, the computed values are all larger than the stability index of extant *Nautilus* (~0.05 [40]), suggesting that living *Nipponites* probably was not able to significantly modify its own apertural orientation (in terms of its vertical orientation). The highest stability in ectocochleates occur in orthocones, especially those without cameral deposits [36, 40]. Lower stability values should occur for morphotypes with larger body chambers that wrap around the phragmocone (e.g., serpenticones [6, 47, 49]). At first glance, *Nipponites* seems to fall into this latter category at later ontogenetic stages because of the series of alternating U-bends surrounding the earlier crioconic phase and somewhat large body chamber. However, the sigmoidal soft body (which heavily influences the total mass distribution) actually appears to be somewhat confined in the vertical directions (Figs 5 and 6). That is, most of the soft body is still distributed below the phragmocone, lowering the center of mass relative to the center of buoyancy and increasing hydrostatic stability. In most cases, uncoiling of the shell tends to generally increase hydrostatic stability compared to planispiral ectocochleates [20, 36, 37, 39, 45, 77].

Due to sufficient hydrostatic stability throughout ontogeny, fixed static orientations are assumed by living *Nipponites mirabilis*. That is, upward to horizontally facing orientations are preferred, while downward facing orientations were not observed in any of the examined ontogenetic stages (Fig 7). These observed orientations may have accommodated a lifestyle of feeding upon small prey in the water column, which has been proposed for other nostoceratid heteromorphs [37, 45, 78]. There is some period of time between about 20% and 40% of the lifespan of *Nipponites mirabilis* (after the crioconic phase and prior to the establishment of regularly alternating U-bends) where orientation oscillates between upward facing and horizontally facing. These somewhat rapid changes may have been an awkward time for these living heteromorphs. On the other hand, this irregularity infers that *Nipponites* was able to assume a functioning lifestyle regardless of these particular differences in orientation. This indifference further suggests that this heteromorph assumed a low energy lifestyle that does not demand athletic predation or predator evasion.

If the ribs of *Nipponites mirabilis* were not oblique, the static orientation of this species would be about 10° less (downward) for many of the examined ontogenetic stages (Fig 8). The obliquity of the ribs (which oscillates in magnitude throughout ontogeny [19]), therefore, assists in maintaining a generally horizontal to diagonally upward facing orientation of the soft body. Rib obliquity also suggests that the evasion of downward orientations was required to effectively function for feeding and perhaps locomotion for most stages. Another example of rib obliquity adjusting apertural orientation and growth direction can be observed in certain terrestrial heteromorph gastropods (e.g., *Opisthostoma vermiculum* [79]). However, this likely constrains orientation more for neutrally buoyant ectocochleates than for terrestrial/benthic gastropods.



## Locomotion of *Nipponites mirabilis*

The juvenile crioconic phase of *Nipponites mirabilis* would have been well suited to horizontal backwards movement with minimal rocking due to its low thrust angles and positioning of the hyponome (and thrust vector) relative to the vertical rotational axis (Fig 1A and 1B; Fig 9). Similar hydrostatic properties are likely for criocone morphotypes with similar proportions. Thrust angles decrease throughout ontogeny with some degree of oscillation but remain above  $-40^\circ$ . These thrust angles at later stages suggest that significant amounts of thrust energy would still be transmitted into horizontal backwards movement, though with some degree of rocking. The subzero thrust angles post-crioconic phase result in the point of thrust located below the horizontal rotational axis suggesting that movement would be rather complicated, with oscillations in apertural angles about some horizontal axis and vertical axis, simultaneously. By examining the lever arms (normalized for each ontogenetic stage), the horizontal components of the lever arms are not much lower than the total lever arms, suggesting that rotational torque about the vertical axis during jet propulsion would be significant. After the crioconic phase, the alternating U-bends in the shell allow the thrust vector to be rotated out of alignment with the vertical rotational axis that passes through the centers of buoyancy and mass. This misalignment after the crioconic phase allows rotation about the vertical axis to take place if thrust is produced normal to the orientation of the aperture. However, this rotational thrust angle is not as ideal as in torticonic (helical) heteromorphs like the turrilitids [34] and the intermediate ontogenetic stages of *Didymoceras* [37], which are closer to  $90^\circ$ . Instead, these rotational thrust angles of the post-crioconic stages, fall between pure rotation ( $90^\circ$ ) and pure translation ( $180^\circ$ ) at around  $135^\circ$  (with some amount of variation throughout ontogeny). If the hyponome was able to bend  $45^\circ$  right or left [80], then living *Nipponites* may have been able to select between pure rotational movement and pure translational movement (influenced by some superimposition of chaotic rocking and hydrodynamic drag). This scenario depends upon the largely unknown ammonoid soft body [69, 70] and propulsive mechanisms [68]. If the hyponome was not able to sufficiently bend, then jet thrust for post-criocone phase individuals would be transmitted into a combination of translation and rotation about the vertical axis.

The thrust angles and directional efficiency of movement provide useful information about the locomotion and feeding of living *Nipponites*. The lateral movement (and perhaps dispersal potential) of crioconic juveniles would have been on par with planispiral ammonoids (albeit with higher hydrodynamic drag), but afterwards, movement is complicated and some amount of rocking and rotation would occur. This rotational movement (pirouetting), however, could have been useful in feeding, perhaps improving the amount of space through which the living ammonoid could have searched for and captured small planktic prey. These hydrostatic properties further support a quasi-planktic, low energy mode of life for *Nipponites*.

## Complex heteromorphy in an evolutionary context

Okamoto [81] suggests that *Nipponites* originated from the nostoceratid *Eubostrychoceras* based on comparisons of shell sculpture, early shell morphology, and stratigraphic occurrence. In a theoretical framework, the juvenile crioconic coiling of both *Eubostrychoceras japonicum* and its probable descendent *Nipponites mirabilis* are very similar. After this phase, the former species retains helical coiling throughout most of its ontogeny except for the adult whorl while the latter species alternates sinistral and dextral helical coiling [17–21, 81]. While the details of the rather-sudden appearance of *Nipponites* remain unclear, the simulations of the current study infer significant differences in hydrostatic properties between these two nostoceratid genera. *Eubostrychoceras japonicum* undergoes similar coiling patterns to the nostoceratid,

*Didymoceras*, but has a longer, stretched out helical phase. Earlier hydrostatic simulations [37] reveal that *Didymoceras* was poorly suited for lateral movement, yet adept at rotating about its vertical axis. These properties are likely analogous to *Eubostrioceras*. While *Nipponites* has a similar ability to rotate about its vertical axis after the criocone phase, horizontal to diagonally upwards orientations are assumed instead of the likely downward diagonal orientations of *Eubostrioceras*. For *Eubostrioceras* to attain *Nipponites*-like orientations, its shell would have to coil upwards, compromising its helical coiling. Furthermore, the alternating U-bends in *Nipponites* retain some degree of lateral movement potential. Therefore, the seemingly-aberrant coiling of *Nipponites* might represent adaptations to maintaining preferred orientations and effective directions of locomotion. Perhaps, this morphology was useful to exploit favorable trophic opportunities in the water column [82].

The hydrostatic simulations of *Nipponites mirabilis* also provide a frame of reference for other nostoceratid heteromorphs. *N. occidentalis*, for example, exhibits a larger degree of uncoiling [33], and therefore, may have had higher stability and a larger lever arm for rotation. Similarly, throughout the late Turonian and Coniacian, a larger degree of uncoiling takes place for specimens found in successively younger strata [81]. These specimens cluster into three distinguished morphotypes [81] that may have become more stable and adept at rotation as they progressed through this time interval. Another morphological constraint is the degree of compactness, which may have served as a selective factor in ammonoids [83]. *Nipponites mirabilis* is quite compact, while this feature varies in other species and morphotypes.

### The stigma of heteromorphy

Heteromorph ammonoids have been commonly regarded as bizarre evolutionary experiments or degenerates [8–15], and their unique coiling schemes are enigmatic in terms of their functional morphology and potential modes of life. While the inevitable phylogenetic extinction of heteromorphs (i.e., typolysis) is now rebutted [8], the stigma of this concept has persisted and is further propagated by their seemingly aberrant coiling schemes. Heteromorph ammonoids, however, were very diverse, disparate, and successful throughout the Cretaceous [45, 82, 84–86]. Furthermore, the coiling schemes of several morphotypes of heteromorph ammonoids suggest that they exploited unique solutions to manage the physical properties that constrained their modes of life by modifying their shells to serve primarily as specialized hydrostatic devices [36–39]. Additionally, some heteromorphs may have been released from certain constraints, allowing freedom to experiment. The hydrostatic simulations of the current study reveal that the coiling of *Nipponites*, which seems biologically absurd, does in fact confer an advantage for specific *syn vivo* orientations and with rotational capabilities. As suggested for several heteromorphs, the general mode of life assumed by *Nipponites* may parallel extant cranchid squids, feeding upon small prey as slow, but not immobile, quasi-planktic cephalopods [6, 33, 77, 87].

### Conclusions

Hydrostatic analyses support a quasi-planktic mode of life for *Nipponites mirabilis* with unique forms of movement that could have enabled a planktotrophic feeding strategy. This species and other heteromorphs with similar proportions had the capacity for neutral buoyancy and were not restricted to the benthos. Throughout the ontogeny of *Nipponites*, horizontally facing to upwardly facing soft body orientations were occupied. These orientations were likely preferred for feeding on small plankton in the water column. This behavior is supported by the tendency for rib obliquity to oscillate [19], which was primarily found to upwardly tilt apertural orientations from the direction of shell growth. Somewhat larger hydrostatic stability

values, relative to *Nautilus*, suggest that the vertical component of the apertural orientation would not have significantly changed during locomotion or interaction with external forms of energy. A change in hydrostatics takes place between the juvenile criocone stage and the later stages consisting of alternating U-bends in the shell, specifically regarding the directional propensity for movement. Although the criocone phase of *Nipponites* likely experienced more hydrodynamic drag than planispiral ammonoids of similar size, this morphology was stable, and proficient at backwards horizontal movement. As the alternating U-bends develop, *Nipponites* is better suited for rotational movement about its vertical axis, while possibly maintaining the option to move horizontally backwards by changing the direction of its hyponome. These *syn vivo* physical properties do not support a benthic or immobile mode of life for *Nipponites*. Its forms of movement were likely slow, however, suggesting that *Nipponites* assumed a low energy lifestyle while pirouetting to scan for small prey in the water column. The hydrostatic properties throughout the ontogeny of *Nipponites* contrast with those of its probable ancestor, *Eubostrioceras* [81]. These differences in morphology along with the hydrostatic analyses in the current study infer that the seemingly convoluted coiling scheme of *Nipponites* represents unique adaptive solutions to several hydrostatic constraints, rather than random morphological aberration.

## Acknowledgments

We thank the Palaeontological Society of Japan for making CT scan data of INM-4-346 and other reference specimens available online. We also thank Keita Mori for donating NMNS PM35490. We appreciate Kei Takano for allowing us to image a private specimen used to estimate the body chamber ratio. Thanks to Daisuke Aiba, Tomoki Karasawa, and Takatoshi Tsuji for assistance with the 3D scans of MCM-A0435. Finally, we would like to thank G. Vermeij, C. Klug, and R. Hoffmann for their constructive reviews of the manuscript.

## Author Contributions

**Conceptualization:** David J. Peterman.

**Data curation:** David J. Peterman, Tomoyuki Mikami, Shinya Inoue.

**Formal analysis:** David J. Peterman.

**Funding acquisition:** David J. Peterman, Tomoyuki Mikami, Shinya Inoue.

**Investigation:** David J. Peterman.

**Methodology:** David J. Peterman.

**Project administration:** David J. Peterman.

**Resources:** David J. Peterman, Tomoyuki Mikami, Shinya Inoue.

**Software:** David J. Peterman.

**Supervision:** David J. Peterman.

**Validation:** David J. Peterman.

**Visualization:** David J. Peterman.

**Writing – original draft:** David J. Peterman.

**Writing – review & editing:** David J. Peterman, Tomoyuki Mikami, Shinya Inoue.

## References

1. Matsumoto T. Some heteromorph ammonites from the Cretaceous of Hokkaido. *Mem Fac Sci Kyushu Univ ser D Geol.* 1977; 23: 303–366.
2. Matsumoto T. The so-called Turonian-Coniacian boundary in Japan. *Bull Geol Soc Denmark.* 1984; 33: 171–181.
3. Hirano H. Cretaceous biostratigraphy and ammonites in Hokkaido, Japan. *Proc Geol Ass.* 1982; 93: 213–223.
4. Hasegawa T., Pratt L.M., Maeda H., Shigeta Y., Okamoto T., Kase T., et al. Upper Cretaceous stable carbon isotope stratigraphy of terrestrial organic matter from Sakhalin, Russian Far East: a proxy for the isotopic composition of paleoatmospheric CO<sub>2</sub>. *Palaeogeogr Palaeoclimatol Palaeoecol.* 2003; 189: 97–115. [https://doi.org/10.1016/S0031-0182\(02\)00634-X](https://doi.org/10.1016/S0031-0182(02)00634-X)
5. Yazykova E.A., Peryt D., Zonova T.D., Kasintzova L.I. The Cenomanian/Turonian boundary in Sakhalin, Far East Russia: ammonites, inoceramids, foraminifera, and radiolarians. *New Zealand J Geol.* 2004; 47: 291–320. <https://doi.org/10.1080/00288306.2004.9515057>
6. Westermann G.E.G. Ammonoid life and habitat. In: Landman N.H., Tanabe K., and Davis R.A. (eds.), *Ammonoid Paleobiology. Topics in Geobiology.* 1996; 13: 607–707.
7. Westermann G.E.G., Tsujita C.J. Life habits of ammonoids. in: Savazzi E. (ed). *Functional Morphology of the Invertebrate Skeleton.* Wiley, Chichester; 1999. pp. 299–325.
8. Wiedmann J. The heteromorphs and ammonoid extinction. *Biol Rev Camb Philos Soc.* 1969; 44: 1–563. <https://doi.org/10.1111/j.1469-185x.1969.tb00819.x>
9. Swinnerton H.H. *Outlines of Palaeontology.* London: Arnold; 1930.
10. Dacqué E. *Organische Morphologie und Paläontologie.* Berlin: Borntraeger; 1935.
11. Schindewolf O.H. *Palaontologie, Entwicklungslehre und Genetik.* Berlin: Borntraeger; 1936.
12. Schindewolf O.H. *Darwinismus oder Typrostrophismus?* *Magyar biol. Kut. Munk.* 1945; 16: 104–177.
13. Schindewolf O.H. *Grundfragen der Paläontologie.* Stuttgart: Schweizerbart; 1950.
14. Erben H.K. *Das stammesgeschichtliche Degenerieren und Aussterben.* *A.d. Heimat.* 1950; 58: 116–123.
15. Müller A.H. *Der Grobablauf der stammesgeschichtlichen Entwicklung.* Jena: Fischer; 1955.
16. Yabe H. Cretaceous Cephalopoda from the Hokkaido, Part 2. *Journ Coll Sci Imp Univ Tokyo.* 1904; 20: 1–45.
17. Seilacher, A., Gishlick, A. *Morphodynamics.* Boca Raton, FL; 2015.
18. Okamoto T. Theoretical morphology of *Nipponites* (a heteromorph ammonoid). *Palaeontol Soc Jpn.* 1984; 36: 37–51. [https://doi.org/10.14825/kaseki.36.0\\_37](https://doi.org/10.14825/kaseki.36.0_37)
19. Okamoto T. Developmental regulation and morphological saltation in the heteromorph ammonite *Nipponites*. *Paleobiology.* 1988; 14: 272–286. <https://doi.org/10.1017/S0094837300012008>
20. Okamoto T. Theoretical modeling of ammonoid morphology. In: Landman N.H., Tanabe K., and Davis R.A. (eds.), *Ammonoid Paleobiology. Topics in Geobiology* 13; 1996. pp. 225–251.
21. Okamoto T. Analysis of heteromorph ammonoids by differential geometry. *Palaeontology.* 1988; 31: 37–51.
22. Illert C. *Nipponites mirabilis*: a challenge to seashell theory. *Nuovo Cimento.* 1990; 12: 1405–1421.
23. Diener C. Lebensweise und Verbreitung der Ammoniten. *Neues Jahrb Geol Palaontol Abh.* 1912; 2: 67–89.
24. Berry E. Cephalopod adaptations—The record and its interpretations. *Q Rev Biol.* 1928; 3: 92–108.
25. Schmidt H. Über die Bewegungsweise der Schalencephalopoden. *Paläontol Z.* 1930; 12: 194–208.
26. Moore R., Lalicker C., Fischer A. *Invertebrate fossils.* McGraw-Hill Co., New York; 1952.
27. Tasch P. *Paleobiology of the invertebrates.* J. Wiley and Sons, New York; 1973.
28. Ebel K. Mode of life and soft body shape of heteromorph ammonites. *Lethaia.* 1992; 25: 179–193. <https://doi.org/10.1111/j.1502-3931.1992.tb01383.x>
29. Trueman A.E. The ammonite body chamber, with special reference to the buoyancy and mode of life of the living ammonite. *Q J Geol Soc London.* 1941; 96: 339–383. <https://doi.org/10.1144/GSL.JGS.1940.096.01-04.14>
30. Tanabe K., Obata I., Futakami M. Early shell morphology in some Upper Cretaceous heteromorph ammonites. *Trans Proc Palaeontol Soc Jpn.* 1981; 124: 215–234.
31. Higashiura K., Okamoto T. Life orientation of heteromorph ammonites under the negatively buoyant condition: a case study on the *Eubostrychoceras muramotoi* Matsumoto. *Fossils.* 2012; 92: 19–30.



32. Seilacher A., Labarbera M. Ammonites as cartesian divers. *Palaios*. 1995; 10: 493–506.
33. Ward P., Westermann G. First Occurrence, Systematics, and Functional Morphology of *Nipponites* (Cretaceous Lytoceratina) from the Americas. *J Paleontol*. 1977; 51: 367–372.
34. Klinger H.C. Speculations on buoyancy control and ecology in some heteromorph ammonites. In: House M.R., and Senior J.R., (eds.) *The Ammonoidea*. The Systematics Association, Special Volume No. 18; 1980. pp. 337–355.
35. Okamoto T. Changes in life orientation during the ontogeny of some heteromorph ammonoids. *Palaeontology*. 1988; 31: 281–294.
36. Peterman D.J., Ciampaglio C., Shell R.C., Yacobucci M.M. Mode of life and hydrostatic stability of orthoconic ectocochleate cephalopods: hydrodynamic analyses of restoring moments from 3D-printed, neutrally buoyant models of a baculite. *Acta Palaeontol Pol*. 2019; 64: 441–460. <https://doi.org/10.4202/app.00595.2019>
37. Peterman D.J., Yacobucci M.M., Larson N.L., Ciampaglio C.N., Linn T. A method to the madness: ontogenetic changes in the hydrostatic properties of *Didymoceras* (Nostoceratidae, Ammonoidea). *Paleobiology*. 2020; 46: 237–258. <https://doi.org/10.1017/pab.2020.14>
38. Peterman D.J., Hebdon N., Ciampaglio C.N., Yacobucci M.M., Landman N.H., Linn T. Syn vivo hydrostatic and hydrodynamic properties of scaphitid ammonoids from the U.S. Western Interior. *Geobios*. 2020; 60: 79–98. <https://doi.org/10.1016/j.geobios.2020.04.004>
39. Peterman D.J., Shell R.C., Ciampaglio C.N., Yacobucci M.M. Stable hooks: biomechanics of heteromorph ammonoids with U-shaped body chambers. *J Molluscan Stud*. 2020; forthcoming. <https://doi.org/10.1093/mollus/eyz035>
40. Peterman D.J., Barton C.C., Yacobucci M.M. The hydrostatics of Paleozoic ectocochleate cephalopods (Nautiloidea and Endoceratoidea) with implications for modes of life and early colonization of the pelagic zone. *Palaeontol Electron*. 2019; 22.2.27A: 1–29. <https://doi.org/10.26879/884>.
41. Hoffmann R., Lemanis R., Naglik C., Klug C. Ammonoid Buoyancy. In: Klug C, Korn D, De Baets K, Kruta I, Mapes R.H. (eds.), *Ammonoid Paleobiology*. Volume I: From Anatomy to Ecology. Topics in Geobiology. 2015; 43: 611–648.
42. Monks N., and Young J.R. Body position and the functional morphology of Cretaceous heteromorph ammonites. *Palaeontol Electron*. 1998; 1: 1–15. <https://doi.org/10.26879/98001>
43. Kaplan P. Biomechanics as a test of functional plausibility: testing the adaptive value of terminal-count-down heteromorphy in Cretaceous Ammonoids. *Jahrb Geol Bundesanst*. 2002; 57: 751–763.
44. Lukeneder A. Ammonoid Habitats and Life History. in: Klug C., Korn D, De Baets K., Kruta I., Mapes R. H. (eds.) *Ammonoid paleobiology, volume I: from anatomy to ecology*. Topics in geobiology. 2015; 43: 689–791.
45. Hoffmann R., Slattery J., Kruta I., Linzmeier B., Lemanis R.E., Mironenko A., et al. Recent advances in heteromorph ammonoid paleobiology. *Biol Rev*. 2020; in review.
46. Raup D.M., Chamberlain J.A. Equations for volume and center of gravity in ammonoid shells. *J Paleontol*. 1967; 41: 566–574.
47. Saunders W.B., Shapiro E.A. Calculation and simulation of ammonoid hydrostatics. *Paleobiology*. 1986; 12: 64–79. <https://doi.org/10.1017/S0094837300002980>
48. Klug C., Korn D. The origin of ammonoid locomotion. *Acta Palaeontol Pol*. 2004; 49: 235–242.
49. Naglik C., Tajika A., Chamberlain J., Klug C. Ammonoid locomotion. in: Klug C. Korn D., De Baets K., Kruta I, Mapes R. (eds.) *Ammonoid Paleobiology*. From anatomy to ecology, Topics in Geobiology. 2015; 43: 649–688.
50. Chamberlain J.A. Hydromechanical design of fossil cephalopods. In House M.R, and Senior J.R. (eds.), *The Ammonoidea*, Systematics Association, London. 1981. pp. 289–336.
51. Morón-Alfonso D.A. Exploring the paleobiology of ammonoids (Cretaceous, Antarctica) using non-invasive imaging methods. *Palaeontol Electron*. 2019; 22.3.57. <https://doi.org/10.26879/1007>
52. Hoffmann R., Lemanis R.E., Falkenberg J., Schneider S., Wesendonk H., Zachow S. Integrating 2D and 3D shell morphology to disentangle the paleobiology of ammonoids: a virtual approach. *Palaeontology*. 2018; 61: 89–104. <https://doi.org/10.1111/pala.12328>
53. Hoffmann R., Schultz J.A., Schellhorn R., Rybacki E., Keupp H., Gerden, et al. Non-invasive imaging methods applied to neo- and paleo-ontological cephalopod research. *Biogeosciences*. 2014; 11: 2721–2739. <https://doi.org/10.5194/bg-11-2721-2014>
54. Lemanis R., Zachow S., Füsseis F., Hoffmann R. A new approach using high-resolution computed tomography to test the buoyant properties of chambered cephalopod shells. *Paleobiology*. 2015; 41: 313–329. <https://doi.org/10.1017/pab.2014.17>

55. Lemanis R., Korn D., Zachow S., Rybacki E., Hoffmann R. The evolution and development of cephalopod chambers and their shape. *PLoS One*. 2016; 11: 1–21. <https://doi.org/10.1371/journal.pone.0151404> PMID: 26963712
56. Tajika A., Naglik C., Morimoto N., Pascual-Cebrian E., Hennhofer D., Klug C. Empirical 3D model of the conch of the Middle Jurassic ammonite microconch *Normannites*: its buoyancy, the physical effects of its mature modifications and speculations on their function. *Hist Biol*. 2015; 27: 181–191. <https://doi.org/10.1080/08912963.2013.872097>
57. Naglik C., Monnet C., Goetz S., Kolb C., De Baets K., Tajika A., et al. Growth trajectories of some major ammonoid sub-clades revealed by serial grinding tomography data. *Lethaia*. 2015; 48: 29–46. <https://doi.org/10.1111/let.12085>
58. Naglik C., Rikhtegar F., Klug C. Buoyancy of some Palaeozoic ammonoids and their hydrostatic properties based on empirical 3D-models. *Lethaia*. 2016; 49: 3–12. <https://doi.org/10.1111/let.12125>
59. Inoue S., Kondo S. Suture pattern formation in ammonites and the unknown rear mantle structure. *Sci Rep*. 2016; 6: 33689. <https://doi.org/10.1038/srep33689> PMID: 27640361
60. Palaeontological Society of Japan, 2019, Digital references of computerized tomography of *Nipponites*. Available at <http://www.palaeo-soc-japan.jp/3d-ammonoids/>. Downloaded January 29, 2020.
61. Raup D.M. Geometric analysis of shell coiling: coiling in ammonoids. *J Paleontol*. 1967; 41: 43–65.
62. White Rabbit Co., Ltd. Molcer 1.51. White Rabbit Co., Ltd., Toshima, Tokyo, Japan; 2019.
63. Autodesk Inc. Meshmixer 3.3. Autodesk Inc., San Rafael, California; 2017a.
64. Blender Online Community. Blender, a 3D modelling and rendering package. Blender Institute, Amsterdam. <http://www.blender.org>; 2017.
65. Autodesk Inc. Netfabb 2017.3. Autodesk Inc., San Rafael, California; 2017b.
66. Peterman D.J. Project: *Nipponites mirabilis* 3D models. [https://www.morphosource.org/Detail/MediaDetail/Show/media\\_id/64314](https://www.morphosource.org/Detail/MediaDetail/Show/media_id/64314). Last modified May 7, 2020. 2020.
67. Witmer L. M. The extant phylogenetic bracket and the importance of reconstructing soft tissues in fossils. In: Thomason J.J. (ed.) *Functional morphology in vertebrate paleontology*. Cambridge University Press, Cambridge; 1995. pp. 19–32.
68. Jacobs D.K., Landman N.H. Nautilus—a poor model for the function and behavior of ammonoids? *Lethaia*. 1993; 26: 1–12. <https://doi.org/10.1111/j.1502-3931.1993.tb01799.x>
69. Klug C., Riegraf W., Lehmann J. Soft-part preservation in heteromorph ammonites from the Cenomanian-Turonian Boundary Event (OAE 2) in the Teutoburger Wald (Germany). *Palaeontology*. 2012; 55: 1307–1331. <https://doi.org/10.1111/j.1475-4983.2012.01196.x>
70. Klug C., Lehmann J. Soft Part Anatomy of Ammonoids: Reconstructing the Animal Based on Exceptionally Preserved Specimens and Actualistic Comparisons. In: Klug C, Korn D., De Baets K., Kruta I., Mapes R.H., (eds.) *Ammonoid paleobiology, volume I: from anatomy to ecology*. Topics in geobiology. 2015; 43: 515–538.
71. Landman N.H., Cobban W.A., Larson N.L. Mode of life and habit of scaphitid ammonites. *Geobios*. 2012; 45: 87–98.
72. Peterman D.J., Barton C.C. Power scaling of ammonitic suture patterns from Cretaceous Ancyloceratina: constraints on septal/sutural complexity. *Lethaia*. 2019; 52: 77–90. <https://doi.org/10.1111/let.1229>
73. Klug C. Life-cycles of Emsian and Eifelian ammonoids (Devonian). *Lethaia*. 2001; 34: 215–233.
74. Hoffmann R., Zachow S. Non-invasive approach to shed new light on the buoyancy business of chambered cephalopods (Mollusca). IAMG 2011 publication, Salzburg. 2011: <https://doi.org/10.5242/iamg.2011.0163:506–516>
75. Greenwald L., Ward P.D. Buoyancy in *Nautilus*. In: Saunders B.W., Landman N.H., (eds.) *Nautilus—the biology and paleobiology of a living fossil*. Springer, Dordrecht; 1987.
76. Cignoni, P., Ranzuglia, G. MeshLab (Version 1.3.3) [Computer graphics software]. Visual Computing Lab—ISTI—CNR Pisa, Italy. Available from <http://meshlab.sourceforge.net/>; 2014.
77. Ward P. Functional morphology of Cretaceous helically-coiled ammonite shells. *Paleobiology*. 1979; 5: 415–422. <https://doi.org/10.1017/S0094837300016912>
78. Kruta I., Landman N.H., Rouget I., Cecca F., Larson N.L. The jaw apparatus of the Late Cretaceous ammonite *Didymoceras*. *J Paleontol*. 2010; 84: 556–560. <https://doi.org/10.1666/09-110.1>
79. Clements R., Liew T., Vermeulen J.J., Schilthuizen M. Further twists in gastropod shell evolution. *Biol Lett*. 2008; 4: 179–182. <https://doi.org/10.1098/rsbl.2007.0602> PMID: 18182365
80. Packard A., Bone Q., Hignette M. Breathing and swimming movements in a captive *Nautilus*. *J Mar Biol Ass UK*. 1980; 60: 313–327.

81. Okamoto T. Comparative morphology of *Nipponites* and *Eubostrychoceras* (Cretaceous Nostoceratids). *Trans Proc Palaeontol Soc Jpn.* 1989; 154: 117–139. [https://doi.org/10.14825/prpsj1951.1989.154\\_117](https://doi.org/10.14825/prpsj1951.1989.154_117)
82. Cecca F., Hypotheses about the role of trophism in the evolution of uncoiled ammonites: the adaptive radiations of the Ancyloceratina (Ammonoidea) at the end of the Jurassic and in the Lower Cretaceous. *Rend Fis Acc Lincei.* 1998; 9: 213–226.
83. Tendler A., Mayo A., Alon U. Evolutionary tradeoffs, Pareto optimality and the morphology of ammonite shells. *BMC Systems Biology.* 2015; 9: 1–12. <https://doi.org/10.1186/s12918-014-0137-8>
84. Mikhailova I.A., Baraboshkin E.Y., The Evolution of the Heteromorph and Monomorph Early Cretaceous Ammonites of the Suborder Ancyloceratina Wiedmann. *Paleontol J.* 2009; 43: 527–536.
85. Seilacher A. Patterns of macroevolution through the Phanerozoic. *Palaeontology.* 2013; 56: 1273–1283.
86. Landman N.H., Goolaerts S., Jagt J.W.M, Jagt-Yazykova E.A., Machalski M. Ammonites on the brink of extinction: diversity, abundance, and ecology of the Order Ammonoidea at the Cretaceous-Paleogene (K/Pg) boundary. In Klug C., Korn D., De Baets K., Kruta I, Mapes R.H., (eds.) *Ammonoid Paleobiology: From macroevolution to paleogeography.* Topics in Geobiology. 2015; 43: 497–553.
87. Packard A. Cephalopods and fish: the limits of convergence. *Biol Rev.* 1972; 47: 241–307. <https://doi.org/10.1111/j.1469-185X.1972.tb00975.x>